NCAR-TN/EDD-74

The Measurement of Air Velocity and Temperature Using the NCAR Buffalo Aircraft Measuring System

D. H. LENSCHOW

June 1972

NATIONAL CENTER FOR ATMOSPHERIC RESEARCH
Boulder, Colorado

PREFACE

Several years ago it was recognized that the development of inertial navigation systems for aircraft would make possible more accurate measurements of air velocity than were previously possible. Combining this improvement in measurement capability with the mobility of aircraft results in a very powerful tool for investigating a variety of atmospheric problems--from measurements of eddy fluxes of heat, moisture, and momentum within a few tens of meters of the earth's surface to measurements of lee wave structure several kilometers above the surface.

The development of the measuring system on NCAR's Buffalo aircraft is a joint effort of NCAR and the Desert Research Institute (DRI), Reno, Nevada. At NCAR, both the Research Aviation Facility and the Laboratory of Atmospheric Science have contributed to its development. DRI's participation is under the direction of J. Telford.

This report does not discuss measurements from all the sensors on the aircraft. Other sensors include a microwave refractometer (from which humidity fluctuations can be obtained), a dew-point hygrometer, an electrochemical ozone sensor, and a variometer (rate-of-climb sensor). Furthermore, the measurements and methods of measurements discussed here are not to be considered complete or absolute. Not only do the sensors change as new and better ways of measuring become available, but in-flight comparisons with other aircraft and with ground-based sensors and wind tunnel and laboratory tests will continue to shed new light on present methods for making airborne measurements.

CONTENTS

FIGURES

1. INTRODUCTION

This report describes methods used to measure air velocity and temperature from an aircraft and their application to the measuring system on the NCAR Buffalo aircraft. The main components of this system are:

- An inertial navigation system (Litton Industries, Inc., Model LN-15D) that provides measurements of airplane acceleration, velocity, position, and angles of attitude. The stabilized platform of the inertial navigation system is located inside the Buffalo's laminated fiber glass nose boom.

- An air sensing probe (shown in Fig. 1) that provides measurements of angles of attack and sideslip, pitot-static pressure, and temperature. The probe is mounted 5 m forward of the airplane nose on a hollow steel tube. The steel tube is supported by the fiber glass nose boom, and the tube's after end is rigidly attached to the outer case of the inertial navigation system platform. Shock and vibration isolators, mounted between the steel tube and the outer fiber glass boom, insulate the platform and probe from aircraft vibrations. The spectra of vertical and lateral probe acceleration during a flight (Fig. 2) indicate that the natural vibration frequency of the probe is about 8 Hz, with harmonics at 16 and 24 Hz. Recently, the outer boom has been stiffened, but the effect of this modification on the probe's vibration spectra has not yet been determined.

- A second pitot-static tube that provides measurements of both static pressure and pitot-static pressure. This pitot tube, which is free to align itself parallel to the airstream, is mounted 2 m forward of one of the wing tips.

In the following sections the equations used to calculate the air velocity components from the inertial system and air sensing probe measurements are derived, use and limitations of the inertial navigation platform are discussed, methods used to calculate true airspeed and static temperature are presented, and errors in measurement and their effect on the calculated atmospheric variables are discussed.

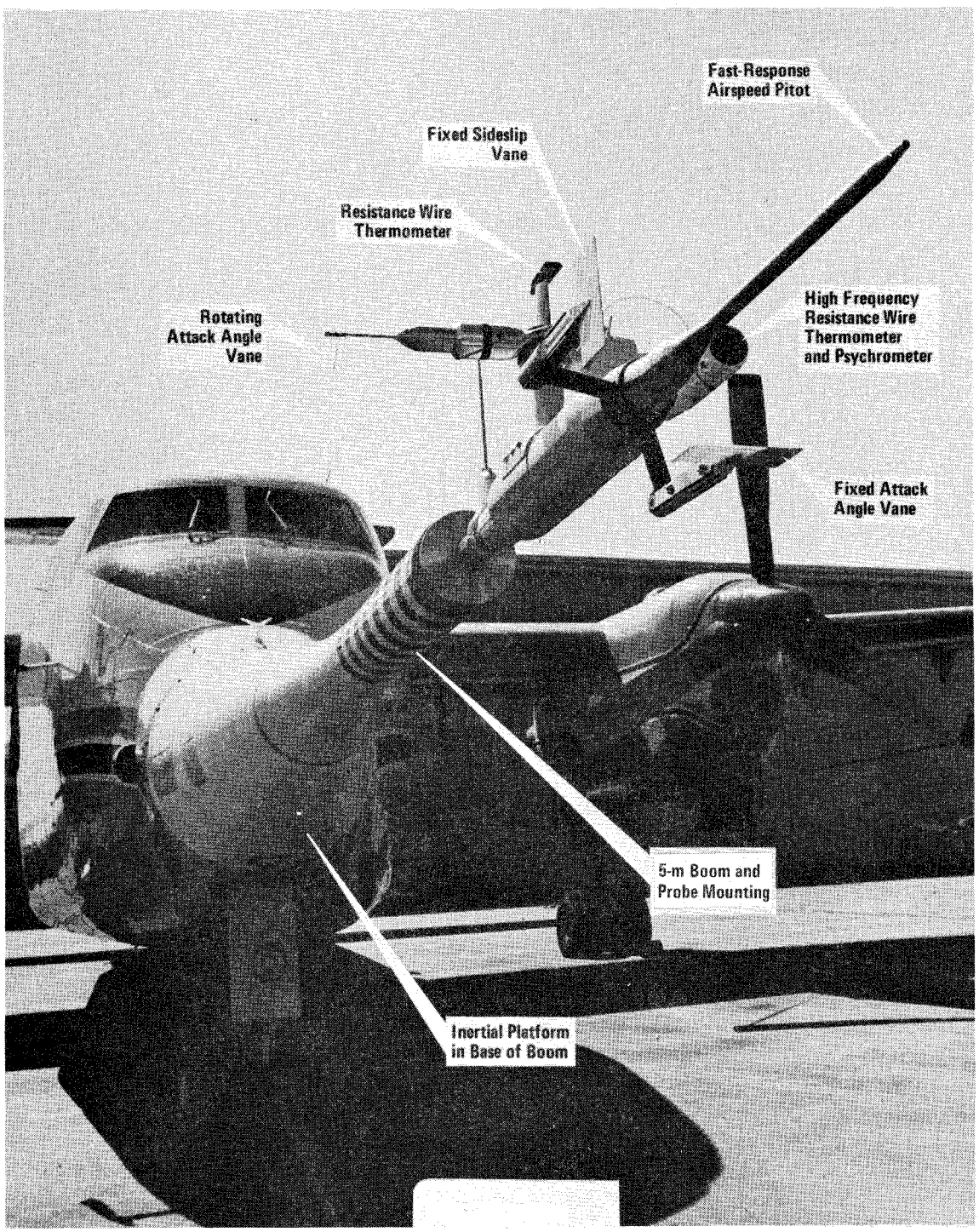

Fig. 1 Flow measurement sensors mounted on the nose boom of the NCAR de Havilland Buffalo aircraft.

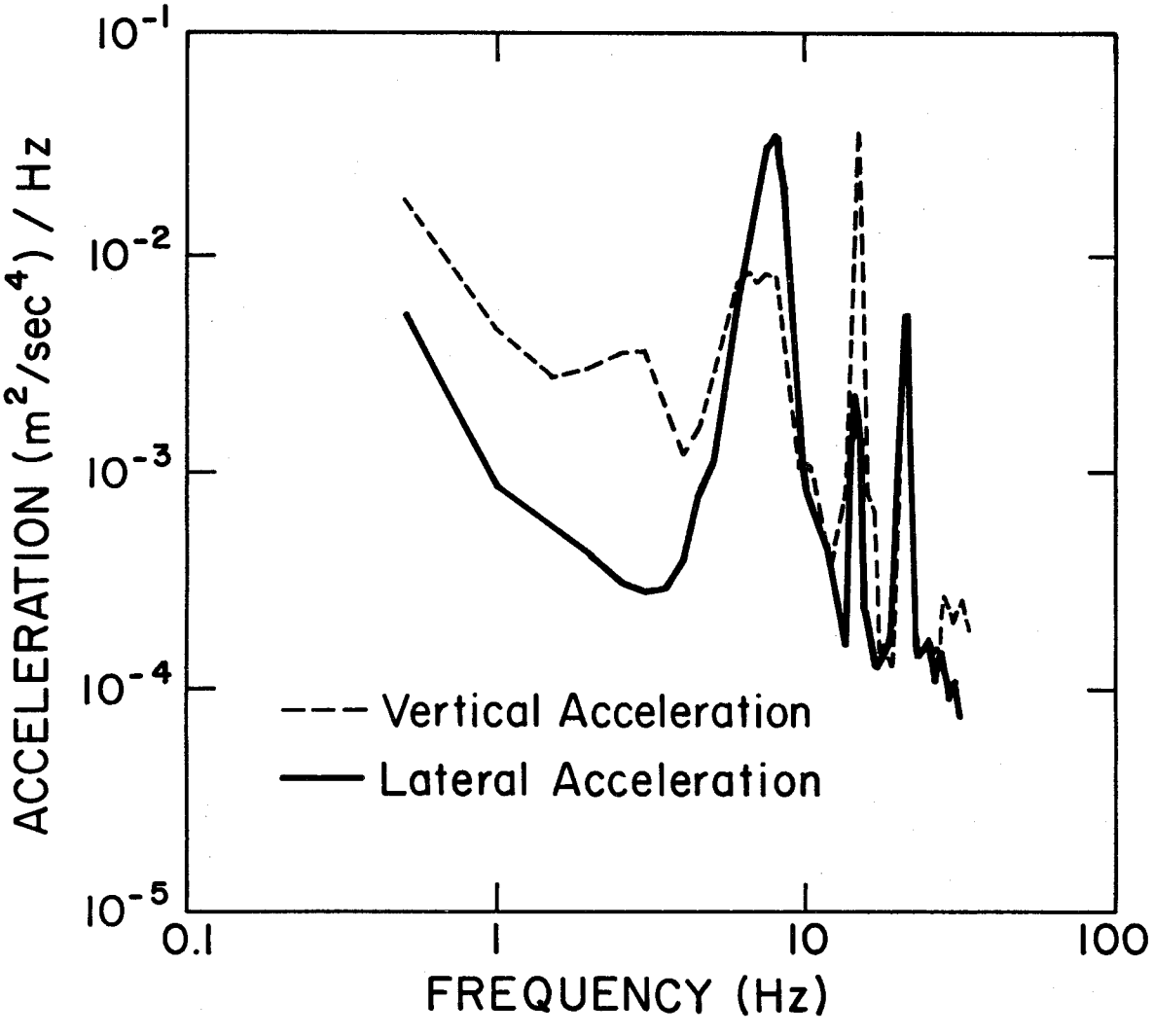

Fig. 2 Spectra of vertical and lateral acceleration of the air sensing probe mounted on the end of the Buffalo nose boom.

2. BASIC VELOCITY EQUATIONS

The derivation of the air velocity equations closely follows Axford (1968). However, several changes were made in terminology and coordinate systems to conform to standard aeronautical engineering usage (Etkin, 1959) for the aircraft coordinate system and to standard inertial navigation (Kayton and Fried, 1969) and meteorological usage for the air velocity in the local earth coordinate system.

The velocity of the air with respect to the earth, $\vec{v} = \vec{i}u + \vec{j}v + \vec{k}w$, is obtained by adding the velocity of the aircraft with respect to the earth, $\vec{v}_p$, and the velocity of the air with respect to the aircraft, $\vec{v}_a$. If all the measurements are made at the same point, we have

$$\vec{v} = \vec{v}_p + \vec{v}_a \tag{2-1}$$

The components of $\vec{v}_a$ are measured with sensors mounted on the aircraft, usually on a boom forward of the aircraft to reduce as much as possible the measurable effects of the distortion of the airflow by the aircraft. The components of $\vec{v}_p$ are obtained from integrated accelerometer outputs on an inertial navigation system or from a radiation transmitting and sensing device such as a doppler radar or radar altimeter.

If the aircraft velocity is obtained from integrated accelerometer measurements, the velocity is measured in an inertial frame of reference. If we convert to an earth-based coordinate system, we obtain

$$\frac{d\vec{v}_p}{dt} = \vec{a} - (\vec{\omega}_p + \vec{\omega}_e) \times \vec{v}_p + \vec{g} \tag{2-2}$$

where $\vec{a}$ is the measured acceleration, $\vec{\omega}_e$ and $\vec{\omega}_p$ are the angular velocities of the earth and platform, respectively, and $\vec{g}$ is the gravitational acceleration (which includes the centripetal acceleration). Since the accelerometers may not be located near the air velocity sensors, the

term $\dot{\vec{\Omega}}_p \times \vec{R}$, where $\dot{\vec{\Omega}}_p$ is the angular acceleration of the aircraft, and $\vec{R} = \vec{i}X + \vec{j}Y + \vec{k}Z$ is the distance from the accelerometers to the air velocity sensors, must be added to Eq. (2-2). Thus, Eq. (2-1) can be combined with the integral of Eq. (2-2) and rewritten as

$$\vec{v} = \vec{v}_a + \int \left[\vec{a} - \left(\vec{\omega}_p + \vec{\omega}_e \right) \times \vec{v}_p + \vec{g} \right] dt + \vec{\Omega}_p \times \vec{R} = \vec{v}_a + \vec{v}_p + \vec{\Omega}_p \times \vec{R} \qquad (2\text{-}3)$$

In the general case, the measured components of $\vec{v}_a$ and $\vec{v}_p$ may not be in the local earth coordinate system. The air sensors, for example, are usually rigidly connected to the aircraft fuselage, or in the case of the Buffalo, rigidly connected to the inertial navigation system. Therefore, it is necessary to know the angles between the coordinates of the measuring systems and the local earth coordinates. The measured velocity components can then be rotated by means of the appropriate angular transformation to the local earth coordinate system. The inertial system on the Buffalo is stabilized along the local earth axes so the rotation angles of the platform gimbals are equivalent to the aircraft attitude angles. From the inside platform gimbal outward, i.e., from the stabilized accelerometer and gyro cluster outward to the aircraft frame, the order of the rotations is as follows: first, a rotation ψ about the z-axis of the earth coordinate system; second, a rotation θ about the y''-axis, which is the y-axis rotated in the horizontal plane by the angle ψ; and third, a rotation ϕ about the x'-axis, which is the x-axis in the aircraft coordinate system. The aircraft axes are shown in Fig. 3; a right-handed angular rotation is positive. The symbols and axes have been defined to correspond to standard aerodynamic conventions (Etkin, 1959).

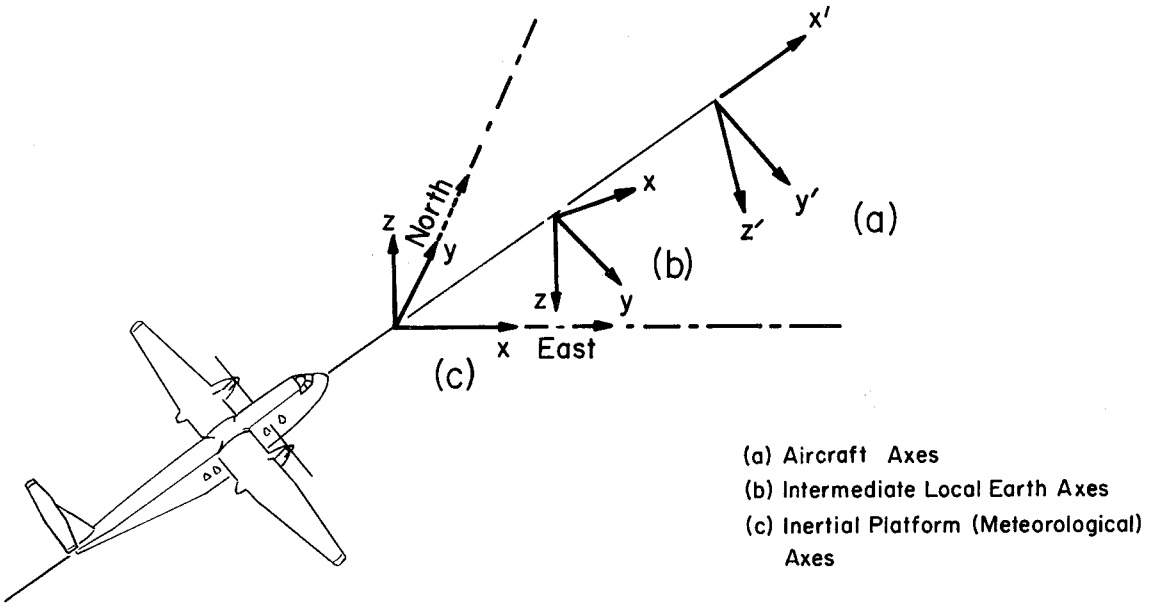

Fig. 3 Coordinate systems used in deriving the equations for calculating the air velocity components.

In matrix notation, the transformation of the air velocity from aircraft (x',y',z') to platform (x,y,z) coordinates [same as (b) coordinates in Fig. 3] is given by

$$\left[u_i\right] = \left[T_{ij}\right] \cdot \left[u'_j\right] \tag{2-4}$$

where

$$\left[T_{ij}\right] = \begin{bmatrix} \cos\psi & -\sin\psi & 0 \\ \sin\psi & \cos\psi & 0 \\ 0 & 0 & 1 \end{bmatrix} \cdot \begin{bmatrix} \cos\theta & 0 & \sin\theta \\ 0 & 1 & 0 \\ -\sin\theta & 0 & \cos\theta \end{bmatrix} \cdot \begin{bmatrix} 1 & 0 & 0 \\ 0 & \cos\phi & -\sin\phi \\ 0 & \sin\phi & \cos\phi \end{bmatrix} \tag{2-5}$$

$$= \begin{bmatrix} \cos\psi\cos\theta & -\sin\psi\cos\phi + \cos\psi\sin\theta\sin\phi & \sin\psi\sin\phi + \cos\psi\sin\theta\cos\phi \\ \sin\psi\cos\theta & \cos\psi\cos\phi + \sin\psi\sin\theta\sin\phi & \sin\psi\sin\theta\cos\phi - \cos\psi\sin\phi \\ -\sin\theta & \cos\theta\sin\phi & \cos\theta\cos\phi \end{bmatrix} \tag{2-6}$$

The terms of $\vec{\Omega}_p \times \vec{R}$ must also be transformed to the local earth coordinate system. In the Buffalo, X is more than an order of magnitude

larger than Y and Z, so that terms involving Y and Z can be neglected. Setting $X = L \simeq 4.3$ m, we have

$$\begin{bmatrix} R_i \end{bmatrix} = \begin{bmatrix} T_{ij} \end{bmatrix} \cdot \begin{bmatrix} L \\ 0 \\ 0 \end{bmatrix} = \begin{bmatrix} L\cos\psi\cos\theta \\ L\sin\psi\cos\theta \\ -L\sin\theta \end{bmatrix} \tag{2-7}$$

Similarly for $\vec{\Omega}_p$, we have

$$\begin{bmatrix} \Omega_{p_i} \end{bmatrix} = \begin{bmatrix} 0 \\ 0 \\ \dot{\psi} \end{bmatrix} + \begin{bmatrix} \cos\psi & -\sin\psi & 0 \\ \sin\psi & \cos\psi & 0 \\ 0 & 0 & 1 \end{bmatrix} \cdot \begin{bmatrix} 0 \\ \dot{\theta} \\ 0 \end{bmatrix} + \begin{bmatrix} \cos\psi\cos\theta & -\sin\psi & \cos\psi\sin\theta \\ \sin\psi\cos\theta & \cos\psi & \sin\psi\sin\theta \\ -\sin & 0 & \cos \end{bmatrix} \cdot \begin{bmatrix} \dot{\phi} \\ 0 \\ 0 \end{bmatrix} \tag{2-8}$$

$$= \begin{bmatrix} -\dot{\theta}\sin\psi + \dot{\phi}\cos\psi\cos\theta \\ \dot{\theta}\cos\psi + \dot{\phi}\sin\psi\cos\theta \\ \dot{\psi} - \dot{\phi}\sin\theta \end{bmatrix}$$

Thus,

$$\vec{\Omega}_p \times \vec{R} = L\Big[\vec{i}(-\dot{\theta}\sin\theta\cos\psi - \dot{\psi}\sin\psi\cos\theta) + \vec{j}\,(\dot{\psi}\cos\psi\cos\theta - \dot{\theta}\sin\psi\sin\theta) - \vec{k}\dot{\theta}\cos\theta\Big] \tag{2-9}$$

The angle of attack, α, is the angle of the airstream with respect to the aircraft in the aircraft's vertical plane, with α positive in the downward direction; the angle of sideslip, β, is the angle of the airstream with respect to the aircraft in the aircraft's horizontal plane, with clockwise (looking from above) rotation positive, as shown in Fig. 4. The air velocity components with respect to the aircraft are calculated by first correcting the measured true airspeed for angle of attack and sideslip sensitivities (see Sect. 4); the magnitude of the corrected true airspeed is defined as U_a. Then the components of air velocity in the aircraft frame of reference are $-U_a\cos\alpha\cos\beta$ along the x'-axis, $-U_a\sin\beta$ along the y'-axis, and $-U_a\sin\alpha$ along the z'-axis; i.e.,

$$\vec{v}_a = -U_a\,(\vec{i}'\cos\alpha\cos\beta + \vec{j}'\sin\beta + \vec{k}'\sin\alpha) \tag{2-10}$$

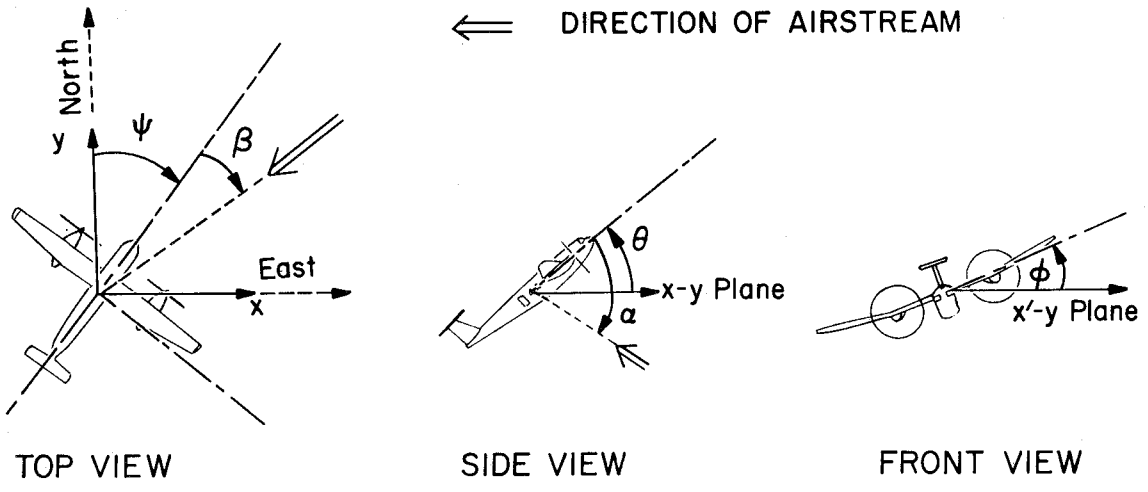

Fig. 4 Airplane attitude angles and axes used in equations for calculating the air velocity components.

So far, the equations have been derived using standard aeronautical engineering terminology. In converting to a meteorological and inertial navigation frame of reference, we make the following changes: first, the sign of vertical velocity is changed so that w is positive in an upward direction; second, ψ, which now corresponds to the true heading, is measured from the y-axis, or from north, and the x-axis now points east, as shown in Fig. 4. As a result, $\psi(\text{new}) = \psi(\text{old}) - 90°$, $u(\text{new}) = -u(\text{old})$, and $w(\text{new}) = -w(\text{old})$. The final equations used for calculating the air velocity with respect to the earth are

$$u = -U_a \left[\cos\alpha\cos\beta\sin\psi\cos\theta + \sin\beta(\cos\psi\cos\phi + \sin\psi\sin\theta\sin\phi) + \sin\alpha(\sin\psi\sin\theta\cos\phi - \cos\psi\sin\phi)\right] + u_p - L(\dot{\theta}\sin\theta\sin\psi - \dot{\psi}\cos\psi\cos\theta)$$

$$v = -U_a \left[\cos\alpha\cos\beta\cos\psi\cos\theta - \sin\beta(\sin\psi\cos\phi - \cos\psi\sin\theta\sin\phi) + \sin\alpha(\cos\psi\sin\theta\cos\phi + \sin\psi\sin\phi)\right] + v_p - L(\dot{\psi}\sin\psi\cos\theta + \dot{\theta}\cos\psi\sin\theta) \qquad (2\text{-}11)$$

$$w = -U_a \left[\cos\alpha\cos\beta\sin\theta - \sin\beta\cos\theta\sin\phi - \sin\alpha\cos\theta\cos\phi\right] + w_p + L\dot{\theta}\cos\theta$$

3. USE OF THE INERTIAL PLATFORM

The aircraft velocity, $\vec{v}_p$, is measured directly from the inertial platform on the Buffalo by summing pulses from a digital rebalance loop on each of the three orthogonally mounted force-balanced accelerometers. The resolution of each pulse is about 0.4 cm sec^{-1}, and the sum is recorded every 0.125 sec. Thus, with the aircraft stationary, the z-accelerometer pulse rate is about 300 pulses per 0.125 sec, which means that successive recorded values of w_p increase by 300 counts.

The computer of the inertial navigation system solves and integrates Eq. (2-2) in the horizontal plane of the local earth coordinate system; thus the instantaneous acceleration, velocity, and position are computed and can be displayed, along with related quantities such as ground speed and drift angle and range and bearing to selected targets or destinations. A block diagram of an inertial navigation system is shown in Fig. 5. The inertial system's computer also calculates the angular velocity required to maintain the platform in a local earth coordinate system. Torque is then applied (by electromagnetic coupling)

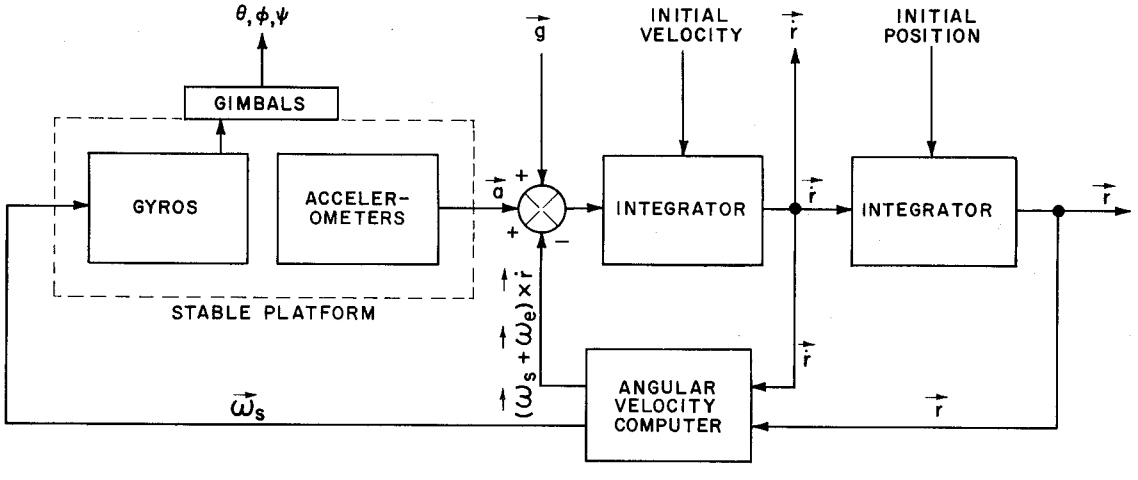

Fig. 5 Block diagram of an inertial navigation system.

to the appropriate gyro axes perpendicular to the spin axes of the gyro. The angular velocity of the gyro rotor along an axis mutually perpendicular to both the gyro spin axis and torque input axis is directly proportional to the applied torque. The axes of the stable platform are slaved to the gyro output axes by rotating the appropriate gimbals so the angular deviation between the two sets of axes is negligible. Thus, the rotation angles of the gimbals are identical to the attitude angles of the aircraft in the local earth coordinate system. These angles are measured with 8-pole resolvers. The two outputs of each of the resolvers are approximately proportional to the sine and cosine of eight times the attitude angle. If we use the pitch angle, θ, as an example,

$$\theta' = \tan^{-1} (E_1/E_2)$$
$$\theta = 0.125 [\theta' + A\sin(2\theta')] \tag{3-1}$$

where E_1 and E_2 are the sine and cosine outputs, respectively, and $A\sin(2\theta')$ is a second harmonic correction ($A < 0.01\theta'$) determined from a laboratory calibration of the resolver. The 400-Hz output voltages of the resolver are demodulated and recorded every 0.0625 sec. Since 8-pole resolvers are used, a 360° rotation of the electrical signal is equivalent to a 45° rotation of the platform angle. Therefore, in processing the data the octant of the angle must be initialized and remembered by the computer. In practice, pitch and roll are always initially referenced to zero and the computer is given an initial octant for determining true heading.

During the analysis of data after a flight, the recorded integrated accelerometer outputs are differentiated, the remaining terms of Eq. (2-2) are calculated, and the equations are integrated; this in effect duplicates part of the real-time computations of the inertial system's computer. The first step in this process is to calculate the effective radii of curvature of the earth, ρ_m and ρ_p, for calculating angular velocity along both the x- and y-axes, i.e., along lines of constant latitude, λ, and constant longitude, ℓ, respectively. The

equations for the reference ellipsoid given by Kayton and Fried (1969) are used; i.e.,

$$\rho_m = \frac{a(1 - \varepsilon^2)}{(1 - \varepsilon^2 \sin^2\lambda)^{3/2}}$$

$$\rho_p = \frac{a}{(1 - \varepsilon^2 \sin^2\lambda)^{1/2}} \tag{3-2}$$

where $\varepsilon^2 = 0.00669566$ and $a = 6378163$ m. The angular velocities along each of the axes are

$$\omega_x = \frac{-v_p}{\rho_m + z}$$

$$\omega_y = \Omega\cos\lambda + \frac{u_p}{(\rho_p + z)} \tag{3-3}$$

$$\omega_z = \Omega\sin\lambda + \frac{u_p \tan\lambda}{(\rho_p + z)}$$

where z is the altitude above sea level and $\Omega = 7.2921151 \times 10^{-5}$ rad $\sec^{-1}$, the earth's angular velocity.

The resulting equations for the components of the time derivative of velocity along each axis are

$$\dot{u}_p = a_x + (\omega_z + \Omega\sin\lambda)\, v_p - (\omega_y + \Omega\cos\lambda)\, w_p$$

$$\dot{v}_p = a_y - (\omega_z + \Omega\sin\lambda)\, u_p + \omega_x v_p \tag{3-4}$$

$$\dot{w}_p = a_z + (\omega_y + \Omega\cos\lambda)\, u_p - \omega_x v_p - g$$

The components of $\vec{v}_p$ are obtained from the integrals of Eq. (3-4).

Latitude (north of the equator) and longitude (west of the prime meridian) are obtained from the integration of

$$\dot{\lambda} = -\omega_x = v_p \Big/ (\rho_m + z)$$
$$\dot{\ell} = -u_p \Big/ [(\rho_p + z)\cos\lambda] \tag{3-5}$$

A complete error analysis of an inertial navigation system is complicated. However, several salient features can be easily demonstrated by considering a simplified two-dimensional case. As an example, we investigate the error propagation of an accelerometer bias error or an angular misalignment of the platform and an accelerometer or gyro drift error, assuming the coriolis terms of Eq. (3-4) can be neglected. The accelerometers along the horizontal axes will sense an acceleration approximately equal to the angular deviation from the local geopotential surface, δ, times g_o, which is the gravitational acceleration at some reference level, R_o, from the center of the earth. The inertial system's computer integrates this acceleration twice, then changes its computed position a distance, ξ, and rotates the platform through an angle ξ/R_o. Thus, the acceleration sensed by the inertial system is

$$\ddot{\xi} = g_o(\delta - \xi/R_o) = -(g_o/R_o)\xi + \varepsilon_x \tag{3-6}$$

where ε_x is the acceleration error.

Along the vertical axis, the gravitational acceleration as a function of the vertical displacement, ζ, away from some reference level and the latitude can be obtained from the equation

$$g(\zeta) = g(1 + \zeta/R_o)^{-2}(1 + 0.00529\ \sin^2\lambda)$$
$$\simeq g_o(1 - 2\zeta/R_o)(1 + 0.00529\ \sin^2\lambda)\ \text{cm sec}^{-2} \tag{3-7}$$

According to Kayton and Fried (1969), this equation is accurate to within 0.02 cm sec^{-2} at sea level. The resulting equations for

horizontal and vertical position errors (neglecting the latitudinal variation of g) are

$$\begin{aligned} \ddot{\xi} + \omega_s^2 \xi &= \varepsilon_x \\ \ddot{\zeta} - 2\,\omega_s^2 \zeta &= \varepsilon_z \end{aligned} \tag{3-8}$$

where $\omega_s = \sqrt{g_o/R_o} = 1.24 \times 10^{-3}$ rad sec^{-1} (equivalent to a period of 84.4 min, known as the Schuler period). The major effect of the neglected coriolis terms involving u_p and v_p, which are typically about 10% of ω_s, is to divide the horizontal error into two sinusoidal components with angular velocities of approximately $\omega_s \pm 1/2(\omega_z + \Omega\sin\lambda)$. Thus, the two sinusoidal components added together result in a modulated error with a carrier frequency of ω_s and a modulation frequency of $1/2(\omega_z + \Omega\sin\lambda)$.

As an example, we assume

$$\begin{aligned} \varepsilon_x = \varepsilon_z &= \begin{cases} 0 & t < 0 \\ a_o + a_1 t & t \geq 0 \end{cases} \\ \xi(0) = \zeta(0) &= \dot{\xi}(0) = \dot{\zeta}(0) = 0 \end{aligned} \tag{3-9}$$

The solutions of Eq. (3-9) for the velocity error are

$$\begin{aligned} \dot{\xi} &= \frac{a_o \sin\omega_s t}{\omega_s} + \frac{a_1}{\omega_s^2} \quad (1 - \cos\omega_s t) \\ \dot{\zeta} &= \frac{a_o \sinh\sqrt{2}\omega_s t}{2\omega_s} - \frac{a_1}{2\omega_s^2} \quad (1 - \cosh\sqrt{2}\omega_s t) \end{aligned} \tag{3-10}$$

As can be seen, the vertical velocity error diverges rapidly. To compare the two errors, we assume $a_o = 2 \times 10^{-2}$ cm sec^{-2} and $a_1 = 2 \times 10^{-5}$ cm sec^{-3}. Substituting these values into Eq. (3-10) we obtain

$$\dot{\xi} = 16 \sin\omega_s t + 13 (1 - \cos\omega_s t) \text{ cm sec}^{-1}$$
$$\dot{\zeta} = 8 \sinh\sqrt{2}\omega_s t - 6 (1 - \cosh\sqrt{2}\omega_s t) \text{ cm sec}^{-1} \qquad (3\text{-}11)$$

These variables are plotted in Fig. 6. The position errors, i.e., the

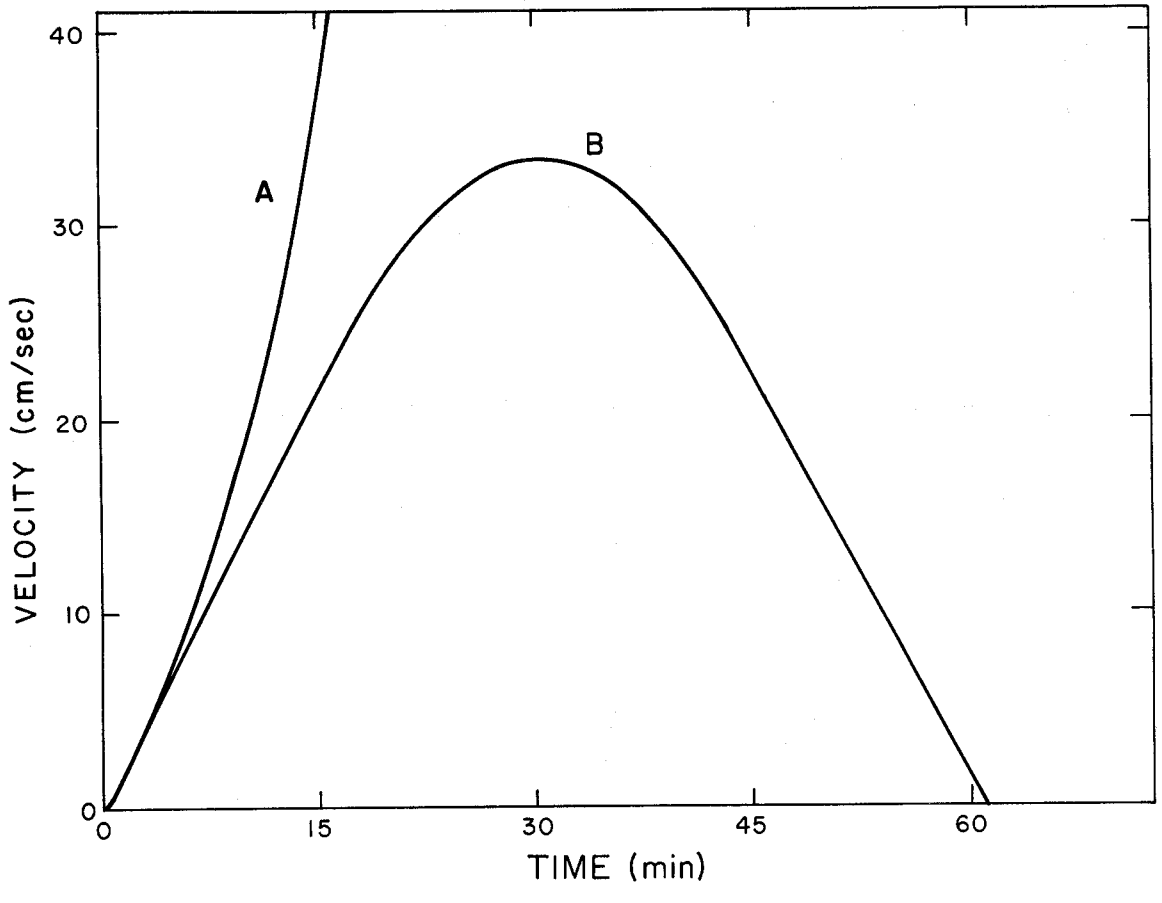

Fig. 6 Velocity errors in an inertial navigation system. (The error generating function is described in text.) Curve A--vertical velocity, Curve B--horizontal velocity.

integrals of Eq. (3-11) are

$$\xi = 130\ [1 - 1.3\ \sin(\omega_s t + 51°) + 10^{-3} t]\ \text{m}$$

$$\zeta = 46\ (\cosh\sqrt{2}\omega_s t - 1) + 37\ \sinh\sqrt{2}\omega_s t - 0.06t\ \text{m} \qquad (3\text{-}12)$$

These variables are plotted in Fig. 7.

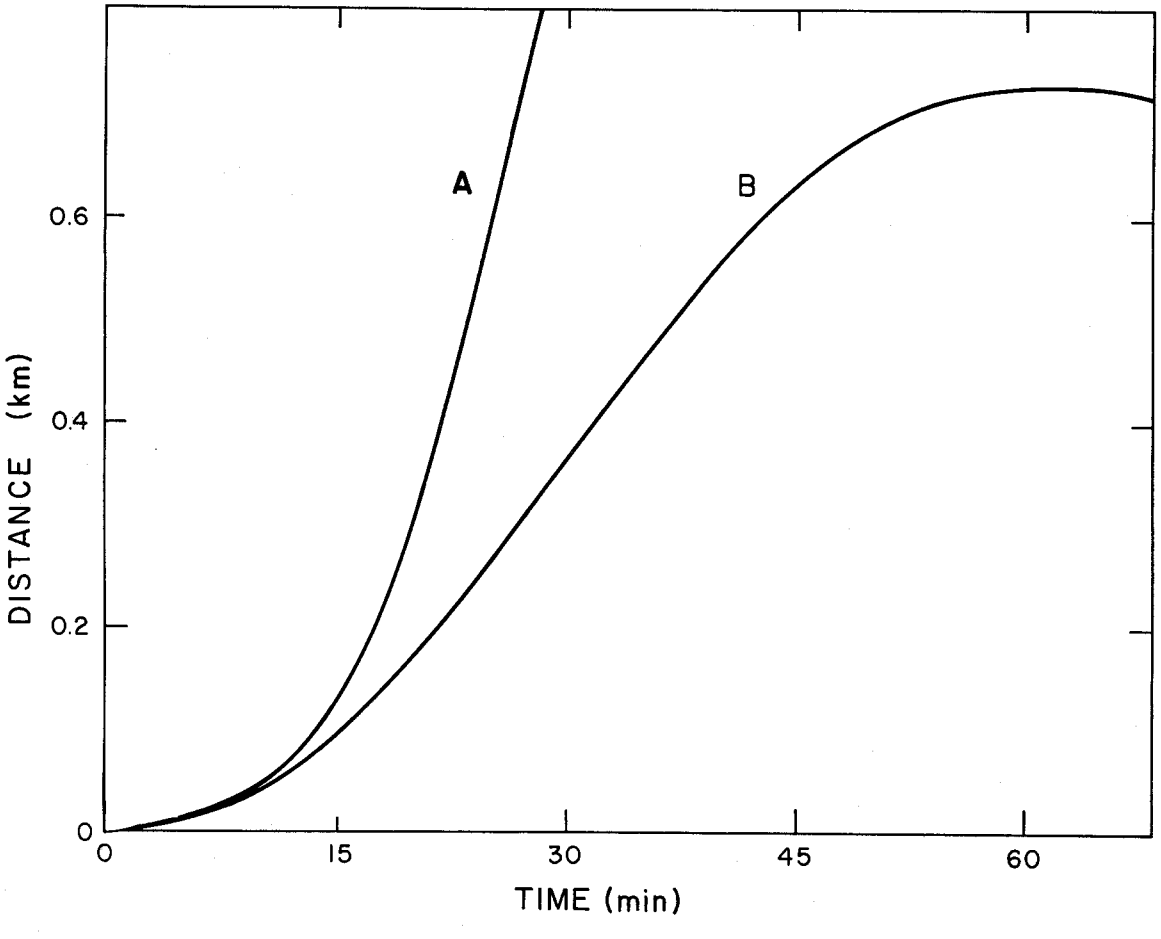

Fig. 7 Position errors in an inertial navigation system. (The error generating function is described in text.) Curve A--inertial altitude, Curve B--horizontal position.

A set of typical errors obtained during flights using the Buffalo's inertial system is shown in Fig. 8. The magnitude of the measured Schuler oscillation error is larger than the assumed error. This is primarily a consequence of the length of the flights. The actual Schuler oscillation error, in contrast to the assumed error, increases with time. In the Appendix a method is outlined for postflight reduction of the inertial system errors.

The magnitude of the angular deviation of the platform from the local vertical, obtained by dividing the first equation of Eq. (3-12) by R_o, adding this result to the second equation of Eq. (3-11), and assuming an aircraft velocity of 100 m sec^{-1}, results in an error in w of

$$0.2 \left[1 - 1.3 \sin(\omega_s t + 51°) + 10^{-3} t\right] + \dot{\zeta} \text{ cm sec}^{-1} \qquad (3\text{-}13)$$

Thus, angular deviations of the platform from the local vertical have a negligible effect on measurements of vertical air velocity.

These results are approximate and are intended primarily to show the types and orders of magnitude of errors present in inertial velocity measurements. [A much more detailed analysis of inertial systems and their errors is made by Broxmeyer (1964).]

The last term of Eq. (3-13) can be made to converge by using a pressure altimeter as an altitude reference. The vertical accelerometer

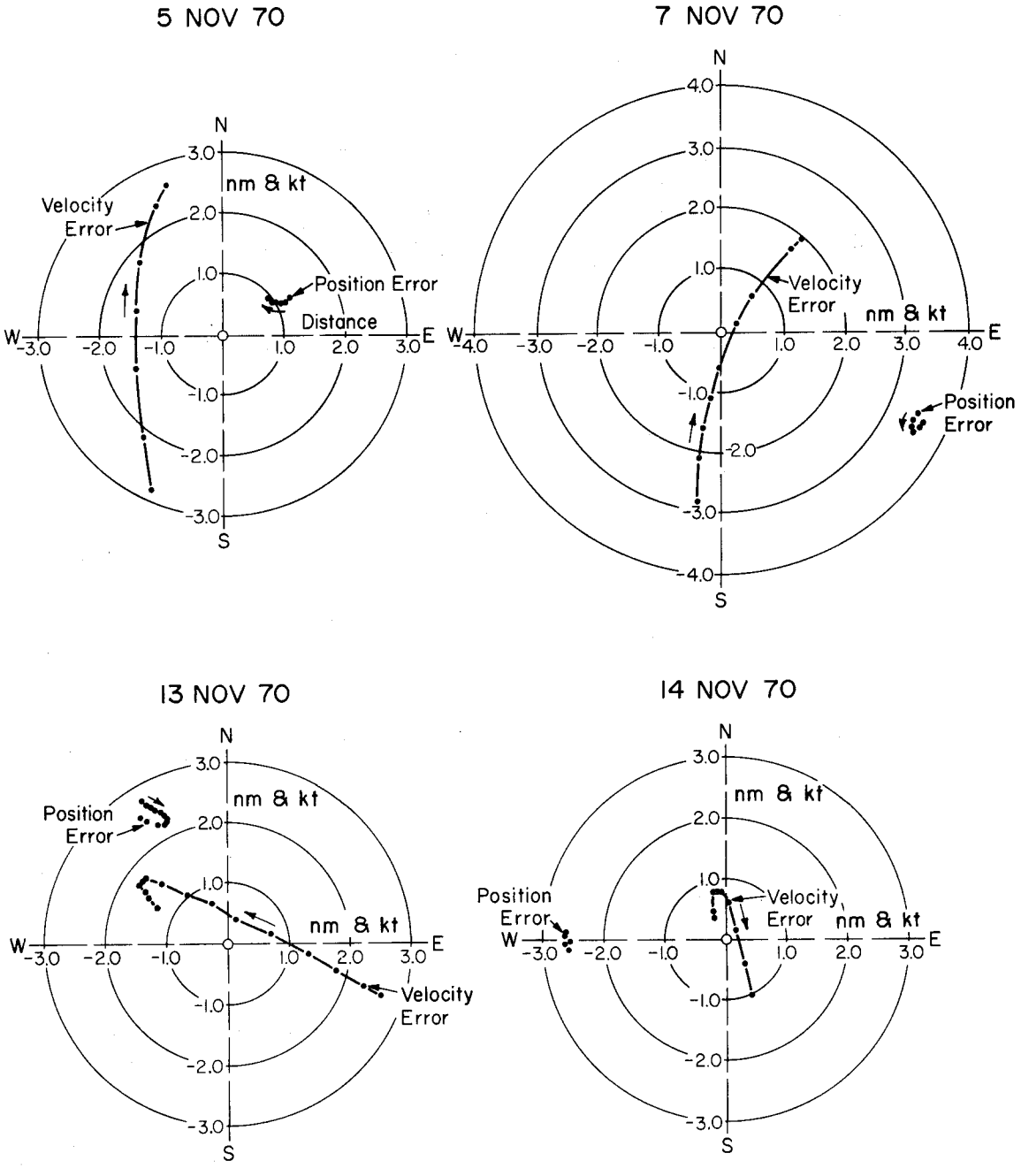

Fig. 8 Position and velocity errors after four flights, each of about 6-hr duration. Total time of each plotted set of errors is about 30 min.

output can be combined, as in Fig. 9, to use the high frequency response of the accelerometer and the low frequency accuracy of the pressure altimeter.

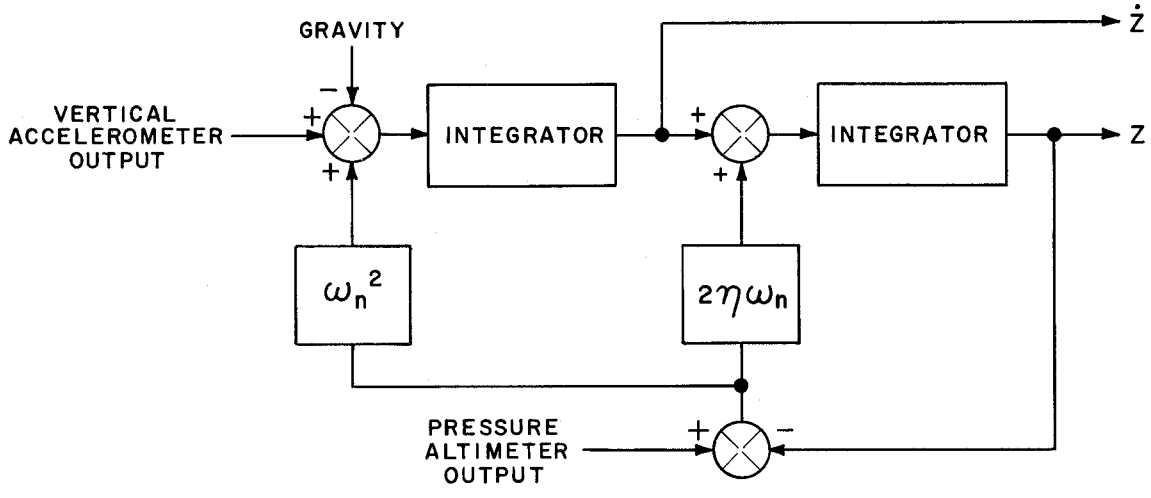

Fig. 9 Block diagram of an inertial barometric vertical velocity and altitude measuring system.

The pressure-stabilized vertical velocity and altitude are obtained from

$$w_p = \int \left[a_z + \omega_n^2 (z_{pa} - z) \right] dt$$
$$z = \int \left[w_p + 2\eta\omega_n (z_{pa} - z) \right] dt \qquad (3\text{-}14)$$

where ω_n is the angular frequency, which determines the high frequency cutoff of the pressure altitude and the low frequency cutoff of the integrated acceleration, and η is the damping ratio, set equal to 0.7. The pressure altitude, z_{pa}, is obtained from the static pressure, using the relation for a constant lapse rate in a dry, perfect gas atmosphere; i.e.,

$$z_{pa} = \frac{T_{os}}{a} \left[1 - \left(P_o / P_{os} \right)^{aR} \right] \qquad (3\text{-}15)$$

where P_{os} and T_{os} are the surface pressure and temperature, respectively,

and a is the lapse rate. In the absence of specific values for a particular flight, P_{os}, T_{os}, and a are set equal to the standard atmospheric values of 1013.25 mb, 288 K, and 0.0065 K m^{-1}, respectively.

The response of Eq. (3-14) to errors in pressure altitude, ε_{pa}, resulting either from errors in measurement or departures of the pressure surface from the geopotential surface, and from errors in measured vertical acceleration, ε_z, can be illustrated in the following way. First, we consider an error in pressure altitude and assume no acceleration; the response is determined from solutions of the equations

$$\begin{aligned} \ddot{z}_p + 2\eta\omega_n\dot{z}_p + \omega_n^2 z_p &= \omega_n^2\varepsilon_{pa} \\ \ddot{z} + 2\eta\omega_n z + \omega_n^2 z &= \ddot{\varepsilon}_{pa} \end{aligned} \tag{3-16}$$

where $\dot{z}_p = \delta w_p$, the vertical velocity error. Next, we consider an error in measured acceleration and no change in pressure; the resulting equations are

$$\begin{aligned} \ddot{z}_p + 2\eta\omega_n\dot{z}_p + \omega_n^2 z_p &= \varepsilon_z + 2\eta\omega_n\int\varepsilon_z dt \\ \ddot{z} + 2\eta\omega_n\dot{z} + \omega_n^2 z &= \varepsilon_z \end{aligned} \tag{3-17}$$

These equations can then be solved for various assumed errors to determine an optimum value for the cross-over frequency, ω_n. An alternative procedure is to solve for z, then set $w_p = \dot{z}$. For the same value of ω_n, this gives a sharper low frequency cutoff for the integrated acceleration and a more gradual decrease in the inclusion of pressure variations in the calculation of w_p above the cross-over frequency. Noise in the recorded signal can change the output of the pressure transducer on the Buffalo as much as ±0.3 mb within 0.25 sec, which is equivalent to a velocity of about ±12 m sec^{-1}. Averaging the signal over several seconds reduces the noise velocity to < 10 cm sec^{-1}.

The value of ω_n used in calculating w_p was obtained in the following way. We transform Eqs. (3-16) and (3-17) to the frequency domain.

At very high frequencies, i.e., $\omega/\omega_n >> 1$, the error in vertical velocity results primarily from noise in the pressure altitude; thus,

$$|\delta w_p| \simeq \varepsilon_{pa}\omega_n^2/\omega \tag{3-18}$$

At very low frequencies, i.e., $\omega/\omega_n << 1$, the error results primarily from drift in the measured vertical acceleration; thus,

$$|\delta w_p| \simeq \varepsilon_z 2\eta/\omega_n \tag{3-19}$$

These errors can be seen in the spectral densities of pressure altitude and inertial altitude (i.e., twice-integrated vertical acceleration) which are in Fig. 10 along with the coherence between these two variables for an 8-min flight leg at nominally constant altitude in very light turbulence. The variables are well correlated only in the region $0.025 < f < 0.15$ Hz. Outside this region, the greater amplitude of the twice-integrated accelerometer output at low frequencies is a result of

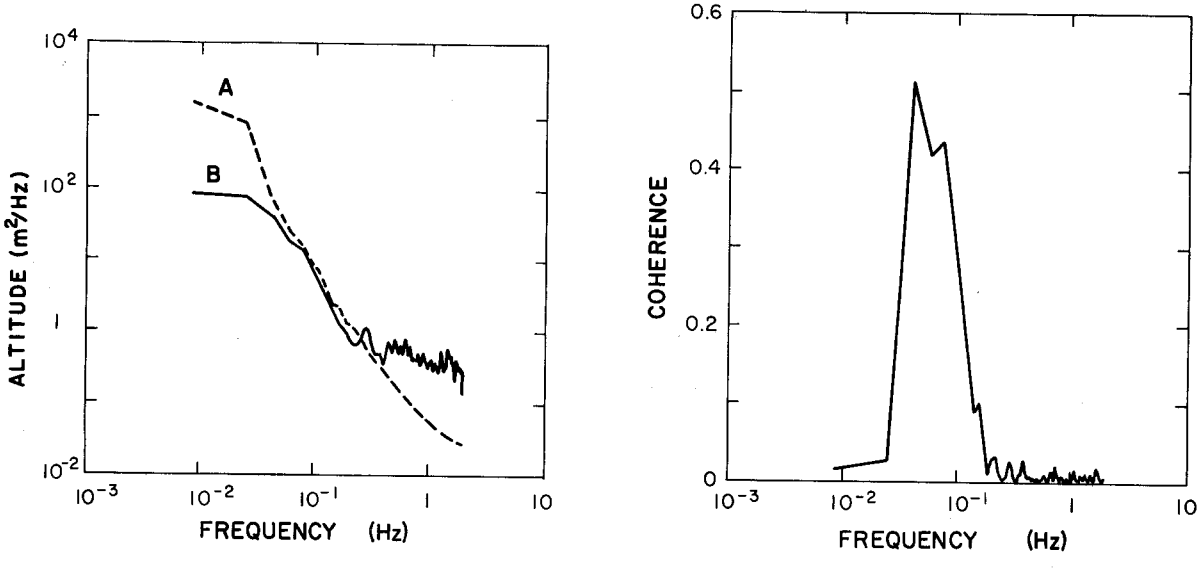

Fig. 10 Left: Spectra of (A) inertial altitude (twice-integrated vertical accelerometer output) and (B) pressure altitude. Right: The coherence of these variables with 34 degrees of freedom.

drift in the accelerometer; the greater amplitude of the pressure altitude at high frequencies is a result of noise in the recorded static pressure output.

The total low frequency (≤ 0.025 Hz) error in vertical acceleration is estimated to be ≤ 2.5 cm sec^{-2}, and the total high frequency (≥ 0.15 Hz) error in pressure altitude is estimated to be ≤ 50 cm. Substituting these values into Eqs. (3-18) and (3-19) we obtain

$$\omega_n = \sqrt[3]{\frac{2\eta\varepsilon_z}{\left(\varepsilon_{pa}/\omega\right)}} = 0.404 \text{ rad sec}^{-1}$$

$$|\delta w_p| \leq 8.7 \text{ cm sec}^{-1} \qquad (3\text{-}20)$$

If we had used $w_p = \dot{z}$, the corresponding errors in vertical velocity would have been $2\omega_n\varepsilon_p$ and $\left(\omega/\omega_n^2\right)\varepsilon_z$ at very high and very low frequencies, respectively. Then we would have had $\omega_n = 0.287$ rad sec^{-1} and $|\delta w_p| = 28$ cm sec^{-1}.

4. AIR SENSING

AIRSTREAM VELOCITY

The three components of airstream velocity are obtained from measurements of the true airspeed and the two angles of the airstream with respect to the aircraft.

The true airspeed of the aircraft, U_a, is calculated from measurements of the pitot-static pressure difference, $q = P_s - P_o$, the static pressure, P_o, and the total air temperature, T_t, using Bernoulli's equation for the conservation of energy of a perfect gas undergoing an adiabatic process,

$$U_1^2/2 + C_p T_1 = U_2^2/2 + C_p T_2 \tag{4-1}$$

where C_p is the specific heat at constant pressure. Applying this equation to the aircraft, $U_2 = 0$, $T_2 = T_t$, $U_1 = U_a$, and $T_1 = T_o$. Thus,

$$U_a = 2C_p\left(T_t - T_o\right)^{1/2} \tag{4-2}$$

For an adiabatic process, $T_o = T_t\left(P_o/P_s\right)^{(\gamma - 1)/\gamma}$, where $\gamma = 1.4$ is the ratio of specific heats for dry air. By substituting this into Eq. (4-2),

$$U_a = \left\{2RT_t\gamma/(\gamma - 1)\left[1 - \left(P_o/P_s\right)^{(\gamma - 1)/\gamma}\right]\right\}^{1/2} \tag{4-3}$$

where

$$R = 2.8704 \times 10^6 \text{ erg g}^{-1} \text{ K}^{-1}. \tag{4-4}$$

Two pitot-static probes are used on the aircraft--one located about 2 m forward of a wing tip and the other (shown in Fig. 1) on the nose boom 5 m forward of the aircraft. The wing-tip probe has a circular stabilizing vane attached to it and is free to align itself in the direction of the airstream, whereas the other probe is fixed to the nose boom. The error in the wing-tip static-pressure measurement was determined by

flying the aircraft past a tower at the same altitude as that of a precision pressure altimeter in the tower at speeds of 59, 82, and 96 m sec^{-1}, which cover the normal speed range of the aircraft. The error in static pressure was measured to be (0.046 ± 0.005) q. Using the measurements reported by Gracey (1958) and Gracey and Scheithauer (1951), we estimated the error caused by the effect of the wing tip to be between 0.01 and 0.02 q. The additional observed error may be caused by the shape of the probe and the upstream effect of the stabilizing vane and the wing-tip boom.

If the error in static pressure were due entirely to a decrease in airspeed at the point at which the static pressure is measured, this would require a reduction in airspeed at that point of about 2.3%. The actual reduction in airspeed at the wing-tip pitot port has not yet been accurately determined. The measured pitot-static pressure, q_m, is used to correct the measured static and pitot-static pressure by the following two equations.

$$P_o = P_o(\text{measured}) - 0.046\ q_m \tag{4-5}$$

$$q = 1.046\ q_m \tag{4-6}$$

The pitot-static pressure difference measured at the front of the nose boom is reduced by about 12% more than the uncorrected value at the wing tip (i.e., the measured nose-boom true airspeed is about 6% less than the uncorrected wing-tip true airspeed). Consequently, the nose-boom probe is used only for high-frequency variations in airspeed and for calculation and correction of airstream incidence-angle measurements. The time response of the nose-boom pitot is about 0.01 sec at sea level, and the resonance of the air in the pitot tube has been damped by means of felt plugs inserted in the static and dynamic pressure lines just in front of the tranducer ports.

Since the nose-boom pitot-static tube (United States Air Force type MA-1) is not aligned to the airstream during flight, a correction, based on wind-tunnel measurements, is made for the angle-of-attack and side-slip sensitivities of the probe. For small angles the pitot-static

pressure, $q = P_s - P_o$, was found to be very nearly a measurement of the magnitude of the total air velocity. As the angles of attack and sideslip increase, the error in the pitot-static pressure measurement is mainly a reduction in static pressure. Therefore, the measured pitot-static pressure increases for increasing airstream angles. The following correction equation, obtained from wind-tunnel data taken at a speed of about 30 m sec^{-1}, is used to correct for airstream angle sensitivity of the pitot-static tube to an accuracy of better than 0.5% for angles between +6 and -6°.

$$q = q_m (1 - 0.0025\alpha - 0.0006125\alpha^2) (1 - 0.0003\beta^2) \qquad (4\text{-}7)$$

The airstream angles are measured in degrees away from the longitudinal axis of the tube. The asymmetery of the angle-of-attack sensitivity is caused by the location of the static pressure holes. The tube has two sets of two holes each--one set at an angle of +37.5° and the other at -37.5° from the bottom of the tube. Thus, the tube is symmetric about the sideslip, or yaw, axis.

The airstream angles are measured with two types of vanes. One is a rotating vane free to align itself with the airstream and the angle is obtained directly from the output of an angle transducer. The other type of vane is constrained from rotating, and the angle is obtained by measuring the force, F, exerted on the vane by the airstream and dividing this force by the corrected pitot-static pressure times the area of the vane, S, times a constant, a; i.e.,

$$\alpha = F/(aqS) \qquad (4\text{-}8)$$

The vane is constrained from rotating by a slotted aluminum beam that has a strain gage mounted on each of its four corners. Applying a downward force on the vane causes the top rear and bottom front gages to lengthen and the other two to contract. The output of the gages, connected as a wheatstone bridge circuit, has been found to be directly proportional to the applied force and to the angle of the airstream for

angles between +8 and -8°. The value of a was measured in a wind tunnel to be (0.0475 ± 0.001) deg^{-1}, and the area of the vane is 51.7 cm^2. Values of the output voltage vs force are obtained by putting weights on the vane. This is done periodically in the field to check the calibration of the vanes. The vane output is also sensitive to acceleration, since the vane is not statically balanced. Thus, the equation used to calculate the angle of attack is

$$\alpha = \left[E - ma_z\right]/q + \alpha_o \text{ deg} \tag{4-9}$$

where E is the vane output (E = 0.407 F mb deg), m is the mass sensitivity [≃ 0.8 (deg mb)/(m sec^{-2})], α_o is the vane misalignment with respect to the axis of the probe (which is referenced to the inertial platform axes), and a_z is measured with an accelerometer mounted in the probe. The frequency response of the constrained vane extends to greater than 100 Hz, but at frequencies greater than about 20 Hz the accelerometer and vane do not necessarily oscillate in phase with each other. Previously, the boom acceleration spectra have had a peak at 24 Hz; consequently, the acceleration response of the vane in the neighborhood of this frequency has not been entirely removed. Recently, the nose boom has been stiffened; however the effect of this on the vibration spectra of the probe has not yet been determined. The frequency response of the rotating vane extends to about 30 Hz. More details of the airstream angle measurements are given by Lenschow (1971).

TEMPERATURE

Static air temperature, i.e., the temperature of the air at zero velocity, can be obtained from Eq. (4-2).

$$T_o = T_t - U_a^2/(2C_p) \tag{4-10}$$

In general, an aircraft thermometer does not measure T_t exactly, but measures the air immediately in contact with the sensing element which has not undergone a pure adiabatic process and therefore has a temperature somewhat less than T_t. The ratio of the temperature difference that the

element actually attains to the adiabatic temperature difference is called the recovery factor, r. Therefore,

$$r = \frac{T_t - T_o}{U_a^2/2C_p} \tag{4-11}$$

For a cylindrical element with its axis normal to the flow, r has been measured to be somewhere between 0.6 and 0.7; the recovery factor of a spherical element has been measured to be about 0.75 (Jacob, 1957; Moffat, 1962).

One of the thermometers on the Buffalo consists of a 1-m length of tungsten wire 0.0025 cm in diameter directly exposed to the airstream, with its axis normal to the flow. The wire is supported by monofilament nylon to reduce as much as possible the effects on the sensor time constant of heat conduction to the supports.

The thermal time constant of a cylindrical temperature sensor with its axis normal to the flow is obtained in the following way. The Nusselt number, N, for a cylinder is defined as the ratio of the film heat transfer coefficient, h (cal cm^{-2} sec^{-1} K^{-1}), to the thermal conductivity, k, divided by the diameter, d. Collis and Williams (1959) have measured N as a function of Reynolds number and obtained the equation

$$N = 0.48Re^{0.51}, \quad 44 < Re < 140 \tag{4-12}$$

where $Re = U_a d/\nu$, and ν is the kinematic viscosity of air. The heat flow from a cylinder of length L is given by $\pi dLh(T - T_t)$, where T is the temperature of the cylinder with a heat flow present. We assume there is no external source of heat so the heat flow is given by the specific heat times the rate of change of temperature with time. The specific heat is $(\pi/4)d^2L\rho c$, where ρ is the density and c is the specific heat per unit mass of the cylinder. Thus,

$$\pi dLh(T - T_t) = (\pi/4)d^2L\rho c dT/dt \tag{4-13}$$

Substituting h = Nk/d and Eq. (4-10) into Eq. (4-11), and approximating the exponent in Eq. (4-2) by 1/2, we have

$$dT/dt = 1.92k\nu^{-1/2}U_a^{1/2}d^{-3/2}(\rho c)^{-1}(T - T_t) \qquad (4\text{-}14)$$

For tungsten, $\rho c = 0.64$ cal cm^{-3} K^{-1}, and for dry air at 1,000 mb and 10 C, $k = 5.97 \times 10^{-5}$ cal cm^{-1} sec^{-1} K^{-1} and $\nu = 0.1437$ cm^2 sec^{-1}. Therefore,

$$dT/dt = 4.74 \times 10^{-4}\ U_a^{1/2}\ d^{-3/2}\ (T - T_t) = 1/\tau\ (T - T_t) \qquad (4\text{-}15)$$

with a wire diameter of 0.0025 cm and at an airspeed of 80 m sec^{-1}, the thermal time constant, τ, of the wire is 0.003 sec.

Several types of errors in addition to a recovery factory error can occur in thermometers of this type. These include: (1) self-heating of the wire by the electrical sensing current, (2) heat transfer by radiation between the wire and its environment, (3) heat transfer by conduction to the supports of the wire, and (4) an increase in resistance (and thus apparent temperature) of the wire resulting from the strain caused by the force of the airstream. These errors are estimated in the following paragraphs.

The heating of the wire by the sensing current can be calculated from the left side of Eq. (4-13). The power dissipated by the wire is given by

$$\begin{aligned} W &= \pi dLh(T - T_t) \\ &= 1.51Lk\nu^{-1/2}(dU_a)^{1/2}(T - T_t) \qquad (4\text{-}16) \\ &= 1.0L(dU_a)^{1/2}(T - T_t)\ \text{mW} \end{aligned}$$

To ensure a temperature rise ≤ 0.1C for the 1-m-long wire considered here, with $U_a = 80$ m sec^{-1}, $W \leq 44$ mW. The resistance, R, of the tungsten wire is about 120 Ω. Therefore, the voltage across the wire should be ≤ 2.3 V. The temperature coefficient of resistivity, $R_o^{-1}\ (\delta R/\delta T)$,

where R_o is the resistance at 0 C, of the tungsten wire was measured to be about 0.004 C^{-1}; therefore, the maximum sensitivity of the element is 9 mV C^{-1}.

The relative magnitude of heat transfer by radiation between the element and its environment can be estimated by calculating the ratio of the film heat transfer coefficient to the radiation heat transfer coefficient, h_R. From the Stefan-Boltzmann law, $h_R = 4\sigma T^3$, where $\sigma = 1.355 \times 10^{-2}$ cal cm^{-2} sec^{-1} K^{-4}. Therefore, for a cylinder normal to the flow with $44 < Re < 140$

$$\begin{aligned} h/h_R &= (Nk/d)/4\sigma T^3 \\ &\simeq 0.615(U_a/d)^{1/2} \end{aligned} \tag{4-17}$$

If we again use the above example, $h/h_R \simeq 10^3$; thus, heat transfer by radiation is negligible.

The effect of heat transfer by conduction to the supports can be estimated by solving the heat conduction equation for a steady-state heat transfer, assuming no radial temperature gradient exists within the wire and that $\partial T/\partial x = 0$ at a distance ℓ away from the support. The temperature at the supports is given by T_1 and halfway between the supports by T_ℓ, and x is the distance away from the support. The solution to this equation, as given by Eckert and Drake (1959), is

$$\frac{T(x) - T_\ell}{T_1 - T_\ell} = \frac{\cosh\, m(\ell - x)}{\cosh\, m\ell} \tag{4-18}$$

where T(x) is the temperature of the wire minus the temperature at $x = \ell$, $m = \sqrt{4Nk/(d^2 k_t)}$, and $k_t = 0.397$ cal cm^{-1} sec^{-1} K^{-1}, the thermal conductivity of tungsten. Substituting Eq. (4-10) into the expression for m,

$$m \simeq 0.03 U_a^{1/4} d^{-3/4} \tag{4-19}$$

For the example given above, $m = 23\ cm^{-1}$. The average temperature over the total length of wire is obtained by integrating Eq. (4-16). The result is

$$\frac{\overline{T} - T_{\ell}}{T_1 - T_{\ell}} = \frac{\tanh m\ell}{m\ell} \tag{4-20}$$

The separation between the supports is 2.5 cm (i.e., $\ell \simeq 1.25$ cm) so the average temperature of the wire differs from the temperature of the wire neglecting conduction by less than 4% of the difference between the temperature of the support and the temperature of the wire at $x = \ell$.

The drag force of the airstream on the wire induces a strain in the wire which increases the measured temperature. The magnitude of this effect is estimated as follows. The drag force is given by

$$D = \frac{1}{2}C_d \ell dq \tag{4-21}$$

The drag force is equal to the stress on the wire times the cross-sectional area of the wire. Therefore, from the definition of Young's modulus, E,

$$\frac{1}{2}C_d \ell dq = 2(\delta\ell/\ell)\pi(d^2/4)E$$

or

$$\delta\ell/\ell = \frac{C_d \ell q}{\pi d E} \tag{4-22}$$

For drawn tungsten wire, $E = 34 \times 10^{11}$ dyne cm^{-2} (Smithells, 1953). The strain gage factor, $(\ell/R)(\delta R/\delta\ell)$, was measured to be 3.5, and the drag coefficient for a cylinder normal to the flow is $C_d \simeq 1.3$ at Re = 140 (Eckert and Drake, 1959). Substituting these values and the temperature coefficient of resistivity into Eq. (4-20), we have

$$\delta T \simeq 7.6 \times 10^{-11} q(\ell/d) \tag{4-23}$$

In the above example, $\ell/d = 10^3$; therefore,

$$\delta T \simeq 0.005\ C \tag{4.24}$$

All of the above errors have been shown to be negligible for the thermometer considered here. The primary remaining uncertainty is the value of the recovery factor which is now known only to about ±0.05. Using a value of r = 0.65 at U_a = 80 m sec^{-1}, this results in a temperature uncertainty of ±0.16 C.

In order to avoid the inaccuracies of determining the recovery factor (and the fragility of an unprotected wire), a probe manufactured by Rosemount Engineering Co. (Model No. 102E2AL) is also used on the Buffalo. This sensor uses a platinum resistance wire 0.0025 cm in diameter and about 26.7 cm in length. The spacing between supports is about 0.36 cm. The sensing element is protected from particles in the airstream by a 90° bend in the housing. Particles in the airstream are assumed to go straight through, whereas the air goes around the corner. The probe is designed to slow the air adiabatically before it reaches the wire to a speed such that any further adiabatic reduction of speed will not appreciably change the air temperature.

Substituting the above values into the equations for errors in temperature measurement, we find that the only significant error is the effect of heat conduction to the supports. The value of m for this wire, using a thermal conductivity for platinum of 0.1664 cal cm^{-1} sec^{-1} K^{-1}, is < 20 cm^{-1}. From Eq. (4-20), the average temperature of the wire is changed by more than 25% of the difference between the temperature of the supports and the temperature of the wire midway between the supports. This causes a "2-time constant" response to a step-function input, as shown in Fig. 11. The initial slope ($\tau \simeq 0.02$ sec) is the characteristic response of the platinum wire; the slope after several tenths of a second ($\tau \simeq 0.6$ sec) is associated with the supporting structure of the wire. Figure 12 is a comparison of the Rosemount thermometer and an exposed resistance-wire thermometer for an aircraft flight in an unstable boundary layer. The Rosemount thermometer output is appreciably different from the output of the unprotected wire thermometer in a region of intense convection. Thus, a rugged, well-protected element of this type responds rapidly to changes in temperature, but is rather slow in reaching the actual value of temperature.

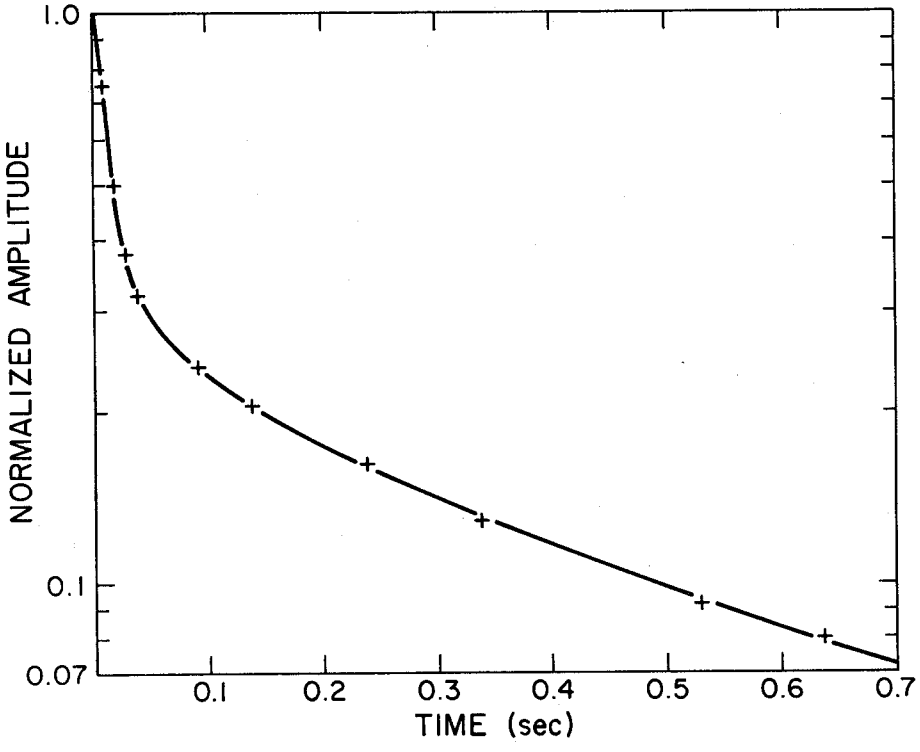

Fig. 11 Response of the Rosemount thermometer (Model No. 102E2AL) to a step-function change in temperature.

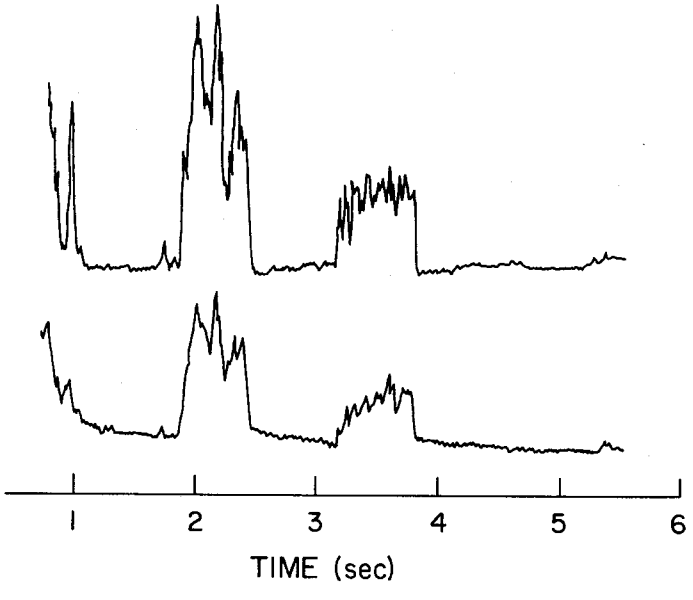

Fig. 12 Comparison of the output of an unprotected resistance-wire thermometer (top) with the Rosemount thermometer (bottom). Amplitude scales for the two sensors are not equal.

CONCLUSION

Although we have discussed the accuracies of sensors on the Buffalo aircraft individually, what is of primary interest is the accuracy of the meteorological variables calculated from the sensor outputs--air velocity and temperature. A further distinction that can be made with air velocity measurements is accuracy of both the mean and variations from the mean.

At the present time, the accuracy of the air velocity measuring system is limited by the accuracy to which the upstream effect of the flow field around the aircraft is known. The transducers now being used on the aircraft for both pitot-static and static pressure measurements can measure pressure to better than 0.05% of the full scale range of the transducer. Although the static pressure can be measured to this accuracy (i.e., 0.5 mb, which is approximately equivalent to 5 m at sea level), this is considerably better than the accuracy to which the upstream effects of the airplane on the pitot-static pressure difference have been determined. At present, the upstream effect is known only to about 2% of the "free stream" pitot-static pressure. At an airspeed of 80 m sec^{-1}, this is an error of 0.8 m sec^{-1}. The horizontal velocity of the aircraft can be measured to at least 0.8 m sec^{-1} by the inertial navigation system, although the addition of some external position or velocity information may be necessary to achieve this, especially for long flights.

An additional source of error for the lateral and vertical components of air velocity is the error in measuring the airstream incidence angles. For lack of better information, if we assume the error in incidence angles is similar in magnitude to the reduction in airspeed at the point at which the measurements are taken (about an 8% reduction), the error in the mean lateral and vertical velocity is < 0.5 m sec^{-1}. (The error in attitude angles obtained from the inertial platform is negligible in comparison with this.) Thus, the three components of the air velocity can be measured from the aircraft with an estimated absolute accuracy of better than 1 m sec^{-1}.

Considering only variations from the mean velocity components (length scales of about 10 km or less), we estimate the longitudinal velocity component to be accurate to 2% and the lateral and vertical components to 8% of the variation (again, because of the upstream effects of the flow around the aircraft) down to a minimum value of about 0.1 m sec^{-1}, which is determined by the accuracy of the pressure and airstream incidence angle tranducers.

The error in temperature, measured on the nose-boom probe, is estimated to be about 0.2 C. This limitation in accuracy is due primarily to the stability of the electronic circuitry now being used. The error in true airspeed does, however, contribute an error of about 0.1 C to the calculated static air temperature. These estimates are consistent with the results of a comparison of tower temperature measurements with aircraft measurements at various speeds at the same altitude and within 100 m of the tower.

Much work still needs to be done, both on more detailed estimation of errors of the present system and on improving the system and modifying the calculations to improve the quality of the measurements. In this sense, this is a status report, and we are continuing to develop and incorporate such improvements in the measurements.

APPENDIX

The errors in the velocity and position obtained from the inertial navigation system can be considerably reduced by using external position and velocity information. Positions may be obtained by recording the time at which the airplane passes over a known geographical location or by using radio navigation. Doppler radar may, under some circumstances, provide additional velocity information. In the simplest case, the position at the beginning and end of a flight are known, and the velocity at these times is zero.

The procedure described here was developed to update the recorded position and horizontal velocity after a flight, using external position and velocity information. We assume that the difference between the corrected and the uncorrected velocity components, u_p' and v_p' $<< (\rho_p + Z)\Omega\sin\lambda$, that $w_p << u_p$ and v_p, and that the product of two differenced quantities is negligible. Then, from Eq. (3-4)

$$\begin{aligned} \dot{u}_p' &= a_x' + f'v_p + fv_p' \\ \dot{v}_p' &= a_y' - f'u_p - fu_p' \end{aligned} \tag{a-1}$$

where $f = 2\Omega\sin\lambda$. To simplify the calculations, we neglect the terms $f'u_p$ and $f'v_p$. If the aircraft returns to its starting point these two terms will, when averaged over the entire flight, be small, although at times during the flight they can sometimes be about as large as fu_p' and fv_p'. Consequently, the corrections obtained from the solution of the resulting equations

$$\begin{aligned} \dot{u}_p' &= a_x' + fv_p' \\ \dot{v}_p' &= a_y' - fu_p' \end{aligned} \tag{A-2}$$

are not always adequate the first time, and sometimes several iterations are necessary to reduce the error sufficiently.

These equations have been applied to the case mentioned above, i.e., the position and velocity errors are assumed to be known at the end of a flight. The functions used for correcting these errors are the first two terms of a polynomial expansion

$$a_x' = a_o + a_1 t$$
$$b_x' = b_o + b_1 t \qquad \text{(A-3)}$$

Substituting Eq. (A-3) into Eq. (A-2) and solving for the position and velocity errors, we obtain the matrix equation,

$$\begin{pmatrix} x_p' \\ y_p' \\ u_p'/f \\ v_p'/f \end{pmatrix} = (A) \cdot \begin{pmatrix} a_o/f^2 \\ a_1/f^3 \\ b_o/f^2 \\ b_1/f^3 \end{pmatrix} \qquad \text{(A-4)}$$

$$(A) = \begin{pmatrix} 1-\cos ft_o & ft_o-\sin ft_o & ft_o-\sin ft_o & f^2t_o^2/2+\cos ft_o-1 \\ \sin ft_o-ft_o & 1-f^2t_o^2/2-\cos ft_o & 1-\cos ft_o & ft_o-\sin ft_o \\ \sin ft_o & 1-\cos ft_o & 1-\cos ft_o & ft_o-\sin ft_o \\ \cos ft_o-1 & \sin ft_o-ft_o & \sin ft_o & 1-\cos ft_o \end{pmatrix}$$

where f in this equation is the coriolis term averaged over the entire flight, of duration t_o. This set of equations has been used to correct the recorded inertial navigation system outputs by solving Eq. (A-4) for a_o, a_1, b_o, and b_1, adding Eq. (A-3) to the first two equations of

Eq. (3-4), and recalculating the horizontal velocity and position of the aircraft. If the resulting errors are still too large, these errors are then used on the left side of Eq. (A-4) and a new set of coefficients a_o, a_1, b_o, and b_1 are calculated. In practice, iterations are usually unnecessary for flights of less than 4 hr.

If position or velocity fixes have been obtained during the flight, the matrix can be expanded to include them. One way to do this is to divide the flight into time increments between fixes of t_1, t_2, . . . , t_n; then the errors can be specified as

$$\begin{aligned} a_x' &= a_o + a_1 t_1 + a_2 t_2 + \ldots + a_n t_n \\ b_x' &= b_o + b_1 t_1 + b_2 t_2 + \ldots + b_n t_n \end{aligned} \tag{A-5}$$

and Eq. (A-4) can be expanded accordingly.

REFERENCES

Axford, D. N., 1968: On the accuracy of wind measurements using an inertial platform in an aircraft, and an example of a measurement of the vertical mesostructure of the atmosphere. *J. Appl. Meteor. 7*, 645-666.

Broxmeyer, C., 1964: *Inertial Navigation Systems*, McGraw-Hill Book Co., New York, N.Y., 254 pp.

Collis, D. C., and M. J. Williams, 1959: Two-dimensional convection from heated wires at low Reynolds numbers. *J. Fluid Mech. 6*, 357-384.

Eckert, E. R. G., and R. M. Drake, Jr., 1959: *Heat and Mass Transfer*, McGraw-Hill Book Co., New York, N.Y., 530 pp.

Etkin, B., 1959: *Dynamics of Flight*, John Wiley & Sons, Inc., New York, N.Y., 519 pp.

Gracey, W., 1958: *Measurement of Static Pressure on Aircraft*, National Advisory Committee for Aeronautics Report 1364, 23 pp.

——, and E. F. Scheithauer, 1951: *Flight Investigation of the Variation of Static-Pressure Error of a Static-Pressure Tube with Distance Ahead of a Wing and a Fuselage*, National Advisory Committee for Aeronautics TN 2311, 26 pp.

Jacob, M., 1957: *Heat Transfer, Vol. 2*, John Wiley & Sons, Inc., New York, N.Y., 652 pp.

Kayton, M., and W. R. Fried, 1969: *Avionics Navigation Systems*, John Wiley & Sons, Inc., New York, N.Y., 666 pp.

Lenschow, D. H., 1971: On the measurement of vertical and lateral air velocity from an airplane by means of vanes. *J. Appl. Meteor. 10*, 1339-1343.

Moffat, R. J., 1962: Gas temperature measurement. In *Temperature, Its Measurement and Control in Science and Industry, Vol. 3*, Rienhold Publ. Corp., New York, N.Y., 553-571.

Smithells, C. J., 1953: *Tungsten*. 3rd ed., Chemical Publishing Co., New York, N.Y., 326 pp.